JOC The Journal of Organic Chemistry

Note

pubs.acs.org/joc

Discovery of a Long-Range Perlin Effect in a Conformationally Constrained Oxocane

Ellen Berry,[†,⊥] Gabriel dos Passos Gomes,[‡,⊥] Alex MacLean,[§] Justin R. Martin,[∥] and Paul A. Wiget*[,†]

[†]Department of Chemistry and Biochemistry and [§]Department of Biological and Environmental Sciences, Samford University, Birmingham, Alabama 35229, United States

[‡]Department of Chemistry & Biochemistry, Florida State University, Tallahassee, Florida 32306, United States

[∥]Department of Chemistry, University of Alabama at Birmingham, Birmingham, Alabama 35294, United States

Supporting Information

ABSTRACT: Herein, we present the crystal structure, NMR *J* analysis, and conformational and natural bond order analyses of tricyclic oxocane (**1**), resulting in the discovery of a long-range Perlin effect at C_4 and C_5. The normal Perlin effect (NPE) of Δ^1J_{C-H} = 18.38 Hz at C_5 is the largest to date for a nonanomeric methylene due to an unprecedented through-space n → σ* stabilizing interaction. The NPE at C_4 where Δ^1J_{C-H} = 6.91 Hz is nearly double those found in cyclohexanone.

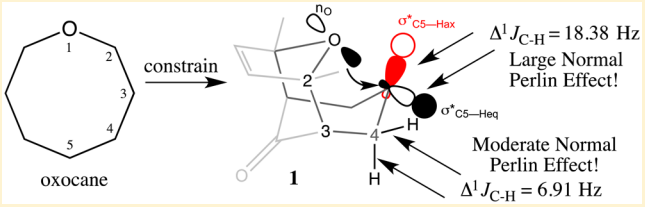

Spin−spin coupling is a key factor in nuclear magnetic resonance (NMR) spectra interpretation. Single-bond C−H spin−spin coupling constants ($^1J_{C-H}$) are used in heteronuclear, indirect-detection NMR experiments such as DEPT, HETCOR, and HSQC. The factors that intrinsically affect single bond C−H coupling constants ($^1J_{C-H}$) are the Fermi contact contribution, the paramagnetic spin−orbit contribution, and diamagnetic spin−orbit contribution.[1] The slight thermal variation in $^1J_{C-H}$ is thought to be a consequence of varying relative conformer populations, not an intrinsic factor affecting its magnitude.[2] Perlin effects (PEs) are observed perturbations in $^1J_{C-H}$ due to electronic donation into localized antibonding orbitals.[3] They are typically used to gauge the donor−acceptor effects surrounding a particular C−H bond when the conformational flexibility has been thermally removed. Once constrained, the difference in axial and equatorial $^1J_{C-H}$ values is calculated via eq 1 to quantify the magnitude of the PEs about a particular carbon.

$$\Delta^1J_{C-H} = |{}^1J_{C-Heq} - {}^1J_{C-Hax}| \quad (1)$$

The terms "normal Perlin effect" and "inverse Perlin effect" have been applied inconsistently in the literature. Though a common usage defines normal and inverse Perlin effects based on whether or not $^1J_{C-Heq} - {}^1J_{C-Hax} > 0$ (likely in order to determine whether C−H or C−C hyperconjugation donors dominate), this definition suffers in remote donor applications and, more importantly, bears no correlation to bond length and s-character, the dominant factors contributing to $^1J_{C-H}$. Herein we define a normal Perlin effect (NPE) as one in which the $^1J_{C-H}$ is inversely proportional to bond length and directly proportional to the degree of s-character and an inverse Perlin effect (IPE) as one in which the $^1J_{C-H}$ is directly proportional to bond length and inversely proportional to the degree of s-character. Ring strain and the various spin−orbit contributions can also strongly affect the magnitude of $^1J_{C-H}$;[4−6] thus, donor−acceptor effects such as the anomeric n → σ* donations and less pronounced effects such as homoanomeric effects, Plough effects, and so-called W-effects have been explored computationally as the origins of observed PEs (see Figure 1).[1,7−18] Therefore, PEs can take on a variety of forms due to the conformation in solution and the presence of heteroatoms, π-systems, or simply aliphatic σ-systems. The donor−acceptor properties of heteroatoms can be observed as much as four bonds away. However, no system has yet been studied that explores through-space donor−acceptor effects that arise *because of* the conformational restrictions in a polycyclic system and the subsequent intraatomic distances and orbital geometries. Herein, we report the observation of such effects resulting the largest NPE to date for a nonanomeric methylene of Δ^1J_{C-H} = 18.38 Hz at C_5 and a truly anomalous NPE at C_4 where Δ^1J_{C-H} = 6.91 Hz, which we dub *angler effects*.

As seen in Figure 2, the conformational rigidity in **1** forces the distant oxygen lone pair over the ring system and in close proximity to the axial H on C_5, five bonds away, and the neighboring methylene groups. This results in C_4−O and C_5−O intramolecular bond distances of 2.942 and 2.782 Å, respectively. The crux of these observations lies in the similarity of the solved crystal structure to the DFT-calculated, energy-minimized, gas-phase structure (B3LYP/6-311+G*). The NMR experiments, NOE, and *J* analysis, in conjunction with the conformational analysis and calculated NMR spectra of the conformers, strongly suggest that the boatlike oxocane structure

Received: April 14, 2016
Published: June 16, 2016

DOI: 10.1021/acs.joc.6b00819
J. Org. Chem. 2016, 81, 5740−5744

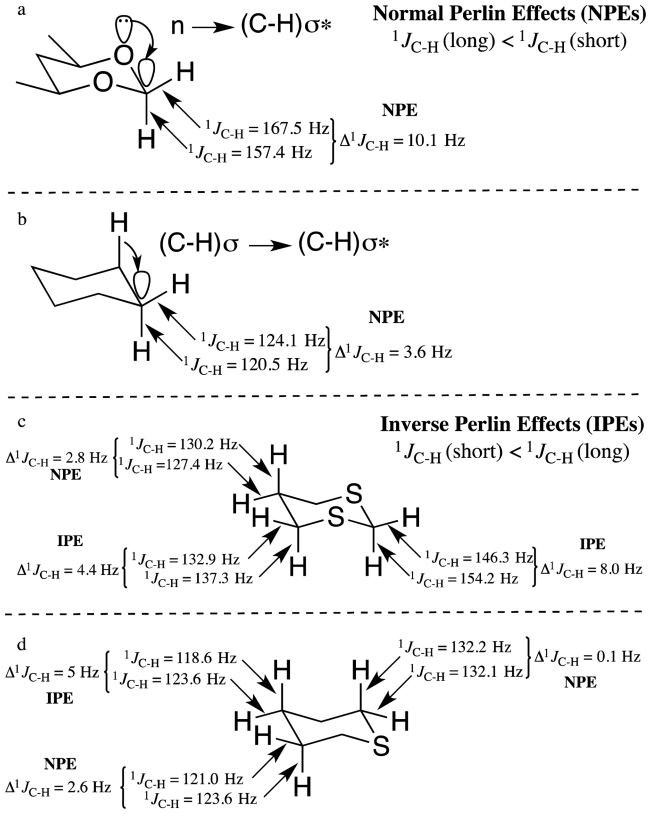

Figure 1. Examples of observed Perlin effects: (a) NPE in a 1,3-dioxane;[16] (b) NPE in cyclohexane;[17] (c) NPE and IPEs in a 1,3 dithiane; (d) NPEs and IPE in a sulfide, showing the influence of the heteroatom four bonds away.[18]

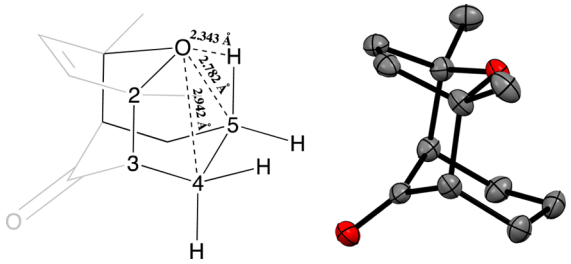

Figure 2. Compound **1**: DFT-calculated intramolecular bond lengths (left) and the solved X-ray crystal structure (right, atomic displacement ellipsoids generated at 50% probability).

shown dominates in solution as well and is therefore responsible for the observed Perlin effects.

The solved crystal structure of this previously unsynthesized [3 + 4] cycloadduct shows the expected *trans* diastereoselectivity in this well-known reaction.[19] It shows the oxocane in a boatlike conformation, with O_1 directed at C_5, and exhibits a C3−C4−C5−C4′ dihedral angle that has contracted considerably to 40.9°.[20] It also shows a slight out-of-plane bend at the carbonyl carbon with a subsequent increase in the O−C(O)−C2 bond angle to 124.1°. Additionally, the C4−C5−C4′ bond angle has widened slightly to 114°, suggesting a slight increase in s-character (vide infra). These combined features suggest the CO-bridged portion of the oxocane has adopted a slight half-chairlike conformation.

The ^{1}H and ^{13}C NMR data are consistent with a symmetrical [3 + 4] cycloaddition structure (see the Supporting Information). The coupled HSQC provided $^1J_{C-H}$. A series of supporting NOE correlations reinforce the proton assignments; however, the methyl protons failed to show an NOE with C5 and thus denied definitive evidence of the C5 orientation in solution. Thus, a *J* analysis was performed to ascertain the degree of conformational flexibility about the C5 methylene. When the Karplus equation is applied to $^3J_{H-H}$ on C4 and C5 in the boatlike oxocane, the estimated dihedral angles align closely with the crystal structure, showing a cyclohexanone with a slightly flattened chair or half-chairlike AA′BB′ coupling pattern. The 13.7 Hz coupling between the signal at δ 2.48 ppm and δ 1.76 ppm is a strong indicator that these two protons are in a predominantly *anti-periplanar* orientation, not *synclinal*. Further, if the chairlike conformer were present, the coupling between C3−H and the protons on C4 would change drastically (see Figure 3). The $^3J_{H-H}$ estimated (1.2 and 4.1

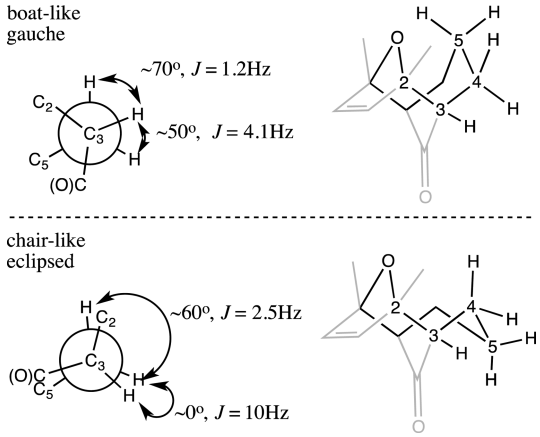

Figure 3. Coupling constants estimated from the DFT-calculated dihedral angles of both conformers.

Hz) by the Karplus equation are in excellent agreement with the experimental results (1.7 and 4.0 Hz), providing strong evidence that the boatlike oxocane dominates in solution.

The preliminary DFT(B3LYP/6-311+G*)-calculated, gas-phase, lowest energy conformation and subsequent conformational analysis, bond length, and NMR estimations correlate with both the crystal structure and the experimental NMR, suggesting a high degree of structural similarities (see the Supporting Information for details). The calculated C5−H_{ax} bond length has contracted and C5−H_{eq} has elongated. The calculated C3−C4−C5−C4′ dihedral angle deviates from the crystal by only 0.39° and the O2−C(O)−C2, by 0.7°. The C4−C5−C4′ bond angle differs by 0.43°. Additionally, a higher energy local minimum was found at 8.15 kcal/mol (relative energy, see the Supporting Information) representing the chairlike oxocane conformation postulated during the *J* analysis. This conformer shows little difference between each of the C−H bond lengths on C4 and C5 and exhibits a much larger C3−C4−C5−C4′ dihedral angle, thus poorly correlating with the experimental data.

The NMR spectrum for each conformation was calculated and can be found in the Supporting Information. A chemical shift comparison for the C5 protons of the two calculated NMR spectra and the experimental spectra are given in Table 1. The chairlike conformer estimates the chemical shifts of the C5 protons to be less than 0.5 ppm apart with both protons being further downfield than the methyl signal yet upfield from the remaining aliphatic resonances. The boatlike conformer places

DOI: 10.1021/acs.joc.6b00819
J. Org. Chem. 2016, 81, 5740−5744

Table 1. Calculated vs Experimental Chemical Shifts in 1

	δ		
	1	boatlike (Δ)	chairlike (Δ)
H_{ax}	2.48	2.85 (0.37)	1.6 (0.88)
H_{eq}	1.13	1.28 (0.15)	1.75 (0.62)
CH_3	1.15	1.4 (0.25)	1.3 (0.15)

the C5 protons nearly 2 ppm apart, with the equatorial signal being upfield from the methyl resonance and the axial signal being downfield from all other aliphatic signals, thus best approximating the experimental NMR.

The observation of these Perlin effects is made clear by comparing the oxocane C−H couplings with those of known and previously analyzed molecules. The cyclohexanone portion of **1** can be compared to cyclohexanone directly to show how the natural conformational restriction and the presence of the oxocane oxygen are changing the coupling constants and PEs. Table 2 compares the observed Perlin effects in **1** (bond lengths calculated at the M06-2X(D3)/6-311++G(d,p)/(SMD = benzene) level of theory) to those adapted from Cuevas and Juaristi[8] when cyclohexanone is cooled to −110° to freeze out the ring-flip process. This figure shows very large NPE at C5 for **1**, and a drastic change (compared to cyclohexanone) in the absolute values of the two $^1J_{C4-H}$, results in a larger NPE of 6.91 Hz. The drastic differences in PEs suggest a different cause for the perturbation of C−H coupling constants. In the comparative systems, the axial C−H bond is longer, and the molecules exhibit a moderate PEs at the positions analogous to C5 in **1**; however, both cyclohexanone and tetrahydropyran show IPEs. Tetrahydropyran provides an example to see how the Perlin effect changes with the location of the heteroatom, showing both a small PE and a modest IPE at carbons 3 and 4, respectively. The PE at C4 of THP is similar to that observed in oxocane **1** for the same relative position but is now an IPE. This is a fascinating result as the dominant pyran conformer would be a chair, though the orientation of the oxygen in **1** to C4 resembles a boat. Both dioxane (Figure 1a) and dithiane (Figure 1c) provide NPEs of modest magnitude; however, both exhibit a dominant anomeric effect as the cause. The $^1J_{C4-H}$ values are interesting as the bond lengths are clearly not the dominant contributor the PEs. These observations reinforce that this locked conformation and the resulting the orbital interactions and effect on hybridization (degree of s-character) need to be better understood.

To explore the origin of these PEs through space, a natural bond orbital (NBO) analysis[21] was performed at the M06-2X(D3)/6-311++G(d,p)/(SMD = benzene) level of theory on **1** as well as on a truncated oxocane, **2**. As seen in Table 3, the oxygen lone pair in both **1** and **2** is involved in a stabilizing through-space interaction with the σ* of C5−H_{eq}, resulting in the expected bond elongation, and concomitant decrease in s-character when compared to C5−H_{ax}. Both **1** and **2** show the oxygen lone pair orthogonal to the σ* of C5−H_{ax} and, thus, are incapable of any stabilizing effect such as improper hydrogen bonding[21,22] (see the Supporting Information for details). However, the proximity of the oxygen to C5−H_{ax} polarizes the C−H bond due to the strong steric factor, resulting in a dramatic decrease in C5−H_{ax} bond length compared to cyclohexanone and THP and accounting for the increase in s-character of the C5−H_{ax} bonding orbital consistent with Bent's rule.[23,24] Considering the interesting PEs on C4, no orbital interactions associated with the oxygen lone pair were found on either **1** or **2**. The nearly identical $^1J_{C5\text{-}Hax}$ and $^1J_{C4\text{-}Heq}$ values are surprising considering the vastly different bond lengths. However, they exhibit identical hybridization ($sp^{3.4}$, see the Supporting Information). Additionally, the C5−H_{eq} and C4−H_{eq} bond lengths are nearly identical but exhibit vastly different $^1J_{C-H}$, suggesting that the difference in hybridization is as important as the donor−acceptor effects observed. Though further work is required, we postulate that in conjunction with the strong oxygen field effects influencing hybridization, the sterically driven C5−H_{ax} bond-length reduction is forcing a greater degree of hyperconjugation into the neighboring methylene. We are currently synthesizing a small library of compounds to discover the nuances of this long-range effect and expect the C4 PEs will be better understood as that data becomes available.

In conclusion, the proposed boatlike conformation of **1** and the resulting location of the oxocane oxygen have allowed the observation of long-range Perlin effects arising from the dangling oxygen over a σ-bond system, producing localized field effects, and a n → σ* stabilizing interaction five bonds from the methylene of observation, which we dub angler effects.

Table 2. Calculated Bond Lengths and Experimental $^1J_{C-H}$ and Perlin Effects[a]

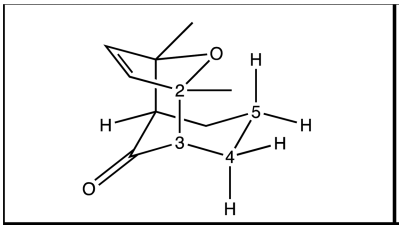

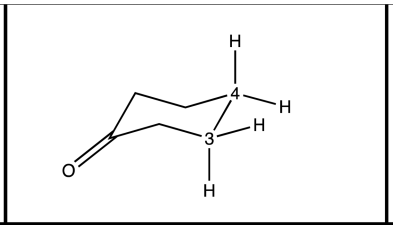

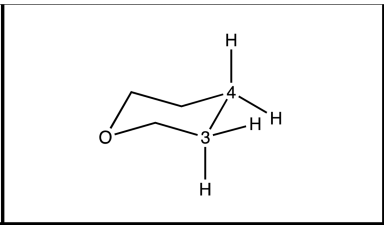

	1				cyclohexanone				tetrahydropyran		
	r(Å)	$^1J_{C-H}$ (Hz)	Δ^1J_{C-H} (Hz)		r(Å)	$^1J_{C-H}$ (Hz)	Δ^1J_{C-H} (Hz)		r(Å)	$^1J_{C-H}$ (Hz)	Δ^1J_{C-H} (Hz)
C_4-H_{ax}	1.0952	134.91	6.91 (N)	C_3-H_{ax}	1.100	122.2	3.9 (N)	C_3-H_{ax}	1.097	122.5	0.6
C_4-H_{eq}	1.0934	141.82		C_3-H_{eq}	1.093	126.1		C_3-H_{eq}	1.097	122.1	
C_5-H_{ax}	1.0879	141.43	18.38 (N)	C_4-H_{ax}	1.099	129.7	4.2 (I)	C_4-H_{ax}	1.099	119	7.2 (I)
C_5-H_{eq}	1.0938	123.05		C_4-H_{eq}	1.096	123.9		C_4-H_{eq}	1.100	126.2	

[a]N = NPE; I = IPE.

DOI: 10.1021/acs.joc.6b00819
J. Org. Chem. 2016, 81, 5740−5744

Table 3. NBO Analysis on 1 and 2

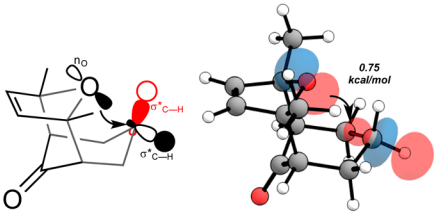

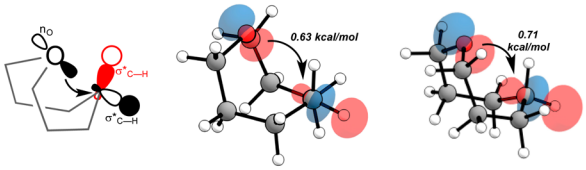

1	M06-2X/6-311++G(D,P)/ (SMD=BENZENE)		2	B3LYP/6-311++G(d,p)		M06-2X/6-311++G(D,P)/ (SMD=BENZENE)	
	Bond Length (Å)	hybridization		Bond Length (Å)	hybridization	Bond Length (Å)	hybridization
C-Heq	*1.0938*	$sp^{3.5}$	C-Heq	*1.097*	$sp^{3.7}$	*1.0953*	$sp^{3.7}$
C-Hax	*1.0879*	$sp^{3.4}$	C-Hax	*1.090*	$sp^{3.5}$	*1.0901*	$sp^{3.5}$
stabilization energy	0.75 kcal/mol		stabilization energy	0.63 kcal/mol		0.71 kcal/mol	

EXPERIMENTAL METHODS

General Methods. All chemicals were used as purchased. Reactions were performed under a static argon atmosphere in a fume hood. Infrared spectra were obtained using a spectrometer equipped with a SMART iTR sampling accessory. All NMR data were obtained using a 700 MHz nuclear magnetic resonance spectrometer equipped with a cryoprobe and ^{13}C cold preamp. Samples were prepared in benzene-d_6 unless otherwise stated. High-resolution mass spectra were acquired on a Orbitrap mass spectometer. Preliminary density functional theory (DFT) calculations at the B3LYP/6-31G* level of theory were performed using Spartan Student v6.1.9. All remaining calculations were carried with the Gaussian 09 software package,[25] using the M06-2X functional[26] with the D3 version of Grimme's dispersion[27] and the 6-311++G(d,p) basis set. The self-consistent reaction field (SCRF) correction was applied through the SMD[28] solvent model for benzene to evaluate solvent effects. Delocalizing interactions were evaluated from M06-2X data with the NBO method, using NBO 3.0 software. NBO analysis transforms the canonical delocalized molecular orbitals from DFT calculations into localized orbitals that are closely tied to the chemical bonding concepts. Each of the localized NBO sets is complete and orthonormal. The filled NBOs describe the hypothetical, strictly localized Lewis structure. The interactions between filled and antibonding orbitals represent the deviation from the Lewis structure and can be used to measure delocalization. For example, delocalizing interactions can be treated via the second-order perturbation energy approach, where n_i is the population of a donor orbitals, F_{ij} is the Fock matrix element for the interacting orbitals i and j, and ΔE is the energy gap between these orbitals. Chemcraft 1.7[29] was used to render the molecules and orbitals.

X-ray Data Collection and Solution. Compound **1** was recrystallized as stated in the synthesis below. A suitable single crystal was mounted on a MicroLoop after coating in Paratone-N oil. Data were collected at the specified temperature with a CCD diffractometer (SMART APEX2) fitted with a low-temperature device. The diffractometer used graphite-monochromated Cu Kα (λ = 1.54178 Å) radiation with a detector distance of 5 cm. The program SAINT was used to collect and reduce the data.[30] Unit cell constants are based upon refinement of the XYZ centroids found using a standard indexing routine (APEX2).[31] The details of the data collection are given in the Supporting Information. All data were corrected for Lorentz and polarization effects and were scaled using the numerical method SADABS.[32] The structures were solved and refined using the Bruker SHELXTL software package.[33] Some of the heavy atoms were found using direct methods, and the remainder were located in difference Fourier maps. Hydrogen atoms were placed in calculated positions with the appropriate molecular geometry δ (C–H = 0.96 Å). The isotropic thermal parameter associated with each hydrogen atom was fixed equal to 1.2 times the U_{eq} value of the atom to which it is bound. Full-matrix least-squares refinement on F^2 was performed on the positional and anisotropic parameters for these atoms.

Synthesis of 1.[34] To a 250 mL round-bottom flask was added a stir bar, 3.09 g of 2-chlorocyclohexanone, 11.19 g (12.6 mL) of 2,5-dimethylfuran, and 123 mL of 2,2,2-trifluoroethanol. To this was added dropwise 5.19 g (7.14 mL) of triethylamine. The reaction was purged with argon, sealed with a septum, and stirred at room temperature for 3 days. Upon return, the reaction was concentrated to approximately 5 mL on a rotary evaporator at 40 °C, dissolved in approximately 50 mL of ethyl acetate (heavy precipitate formed), passed through a pad of silica gel (1 cm deep × 8 cm in diameter), and eluted with ~150 mL of 9:1 hexane/ethyl acetate. The filtrate was concentrated to a slurry on the rotary evaporator at 40 °C. The material was recrystallized from hexanes to afford a total of 2.3 g (50%, unoptimized over two crops) of the expected *trans* diastereomer as colorless needles. Melting point analysis showed a clear and consistent melting range of (79.7 ± 0.2)–(81.0 ± 0.1) °C (three trials each on three different apparatuses; see SI Table 1): ^1H NMR (700 MHz, benzene-d_6) δ 5.71 (s, 2H), 2.48 (qt, J = 13.3, 6.8 Hz, 1H), 2.05 (dd, J = 4.0, 1.7 Hz, 2H), 1.98 (ddt, J = 12.9, 6.4, 1.9 Hz, 2H), 1.76 (dtd, J = 19.1, 6.6, 5.0 Hz, 2H), 1.18 (s, 6H), 1.13 (dddt, J = 13.8, 7.0, 4.5, 2.2 Hz, 1H); ^{13}C NMR (176 MHz, C_6D_6) δ 213.2, 139.5, 128.1, 87.6, 55.1, 29.3, 20.9, 19.7; IR (cm^{-1}) 2970, 2934, 2853, 1722, 1698; HRMS calcd for M + H $C_{12}H_{16}O_2$ + H 193.1223, found 193.1218.

ASSOCIATED CONTENT

Supporting Information

The Supporting Information is available free of charge on the ACS Publications website at DOI: 10.1021/acs.joc.6b00819.

Crystallographic data for **1** (CIF)
NMR and calculation data (PDF)

AUTHOR INFORMATION

Corresponding Author

*E-mail: pwiget@samford.edu.

Author Contributions

$^{\perp}$E.B and D.d.P.G. contributed equally to this work. All authors have given approval to the final version of the manuscript.

Notes

The authors declare no competing financial interest.

ACKNOWLEDGMENTS

We thank the following people at the University of Alabama at Birmingham: Dr. David Graves and Dr. Richard Dluhy, respectively, former and current chairs of the Department of Chemistry for their support and instrument use, Dr. Michael J. Jablonsky for acquiring the NMR data, Dr. Gary M. Gray for

DOI: 10.1021/acs.joc.6b00819
J. Org. Chem. 2016, 81, 5740–5744

allowing us to collaborate with Justin Martin, and Brandon Young and Dr. James A. Mobley for providing the high-resolution mass spectrum at the UAB CCC MS/Proteomics Shared Facility. We appreciate the assistance of Dr. Igor Alabugin at Florida State University for allowing us to collaborate with Gabriel dos Passos Gomes, and we thank Dr. Frank Weinhold of UW—Madison for his helpful conversations. G.d.P.G. thanks IBM for the 2016 IBM Ph.D. scholarship. We also thank the Faculty of the Department of Chemistry and Biochemistry at Samford University for their support and encouragement. This work was funded by the Samford University Howard School of Arts and Sciences research start-up program.

DEDICATION

This work is dedicated to Dr. Stephen D. Starnes for introducing Dr. Wiget to organic chemistry in 2001.

REFERENCES

(1) Cuevas, G.; Juaristi, E.; Vela, A. *J. Phys. Chem. A* **1999**, *103*, 932−937.
(2) Rahkamaa, E.; Jokisaari, J. *Z. Naturforsch., A: Phys. Sci.* **1968**, *23*, 2094−2097.
(3) Wolfe, S.; Pinto, B. M.; Varma, V.; Leung, R. Y. N. *Can. J. Chem.* **1990**, *68*, 1051−1062.
(4) Gil, V. M. S. *Theor. Chim. Acta* **1989**, *76* (4), 291−293.
(5) Muller, N.; Pritchard, D. E. *J. Chem. Phys.* **1959**, *31*, 1471−1476.
(6) Juan, C.; Gutowsky, H. S. *J. Chem. Phys.* **1962**, *37*, 2198−2209.
(7) Suarez, D.; Sordo, T. L.; Sordo, J. A. *J. Am. Chem. Soc.* **1996**, *118*, 9850−9854.
(8) Notario, R.; Roux, V.; Cuevas, G.; Cardenas, J.; Leyva, V.; Juaristi, E. *J. Phys. Chem. A* **2006**, *110*, 7703−7712.
(9) Contreras, R. H.; Esteban, Ä. L.; Diez, E.; Della, E. W.; Lochert, I. J.; dos Santos, F. P.; Tormena, C. F. *J. Phys. Chem. A* **2006**, *110*, 4266−4275.
(10) Alabugin, I. V.; Manoharan, M.; Zeidan, T. A. *J. Am. Chem. Soc.* **2003**, *125*, 14014−14031.
(11) Cuevas, G.; Juaristi, E. *J. Am. Chem. Soc.* **2002**, *124*, 13088−13096.
(12) Wedel, T.; Müller, M.; Podlech, J.; Goesmann, H.; Feldmann, C. *Chem. - Eur. J.* **2007**, *13*, 4273−4281.
(13) Alabugin, I. V. *J. Org. Chem.* **2000**, *65*, 3910−3919.
(14) Garcías-Morales, C.; Martínez-Salas, S. H.; Ariza-Castolo, A. *Tetrahedron Lett.* **2012**, *53*, 3310−3315.
(15) Perrin, C. L.; Armstrong, K. B.; Fabian, M. A. *J. Am. Chem. Soc.* **1994**, *116*, 715−722.
(16) Bock, K.; Wiebe, L. *Acta Chem. Scand.* **1973**, *27*, 2676−2678.
(17) Chertkov, V. A.; Sergeyev, N. M. *J. Am. Chem. Soc.* **1977**, *99*, 6750−6752.
(18) Bailey, W. F.; Rivera, A. D.; Rossi, K. *Tetrahedron Lett.* **1988**, *29*, 5621−5624.
(19) Rigby, J. H.; Pigge, F. C. In *Organic Reactions*; John Wiley & Sons, Inc., 2004.
(20) This angle is an average of the two analogous dihedral angles in the crystal structure, which shows a slight asymmetry in its solved structure.
(21) Weinhold, F.; Landis, C. R. *Discovering Chemistry with Natural Bond Orbitals*; John Wiley and Sons: Hoboken, NJ, 2012.
(22) Alabugin, I. V.; Manoharan, M.; Peabody, S.; Weinhold, F. *J. Am. Chem. Soc.* **2003**, *125*, 5973−5987.
(23) Alabugin, I. V.; Bresch, S.; dos Passos Gomes, G. *J. Phys. Org. Chem.* **2015**, *28*, 147−162.
(24) Clauss, A. D.; Nelsen, S. F.; Ayoub, M.; Moore, J. W.; Landis, C. R.; Weinhold, F. *Chem. Educ. Res. Pract.* **2014**, *15*, 417−434.
(25) Frisch, M. J. et al. *Gaussian 09*, Revision B.01; Gaussian: Wallingford, CT, 2009. The complete reference is found in the SI.
(26) (a) Zhao, Y.; Truhlar, D. G. *Theor. Chem. Acc.* **2008**, *120*, 215. (b) Zhao, Y.; Truhlar, D. G. *Acc. Chem. Res.* **2008**, *41*, 157.
(27) Grimme, S.; Antony, J.; Ehrlich, S.; Krieg, H. *J. Chem. Phys.* **2010**, *132*, 154104.
(28) Marenich, A. V.; Cramer, C. J.; Truhlar, D. G. *J. Phys. Chem. B* **2009**, *113*, 6378.
(29) ChemCraft 1.7 build no. 405, http://www.chemcraftprog.com (accessed Feb 2015).
(30) *SAINT+*, Version V8.34A; Bruker: Madison, WI, 2013.
(31) *APEX2*, Version 2013.10-0; Bruker: Madison, WI, 2013.
(32) *SADABS*, Version 2012/1; Bruker: Madison, WI, 2012.
(33) Sheldrick, G. M. *SHELXL-2013*; Bruker: Madison, WI, 2013.
(34) Cho, S. Y.; Lee, J. C.; Cha, J. K. *J. Org. Chem.* **1999**, *64*, 3394−3395.

DOI: 10.1021/acs.joc.6b00819
J. Org. Chem. 2016, 81, 5740−5744